T. YUKITA
KODAI MATH. J.
42 (2019), 332–357

AN INFINITE SEQUENCE OF IDEAL HYPERBOLIC COXETER 4-POLYTOPES AND PERRON NUMBERS

Tomoshige Yukita

Abstract

In [7], Kellerhals and Perren conjectured that the growth rates of cocompact hyperbolic Coxeter groups are Perron numbers. By results of Floyd, Parry, Kolpakov, Nonaka-Kellerhals, Komori and the author [1], [3], [8], [10], [12], [13], [21], [22], the growth rates of 2- and 3-dimensional hyperbolic Coxeter groups are always Perron numbers. Kolpakov and Talambutsa showed that the growth rates of right-angled Coxeter groups are Perron numbers [9]. For certain families of 4-dimensional cocompact hyperbolic Coxeter groups, the conjecture holds as well (see [7], [19] and also [23]). In this paper, we construct an infinite sequence of ideal non-simple hyperbolic Coxeter 4-polytopes giving rise to growth rates which are distinct Perron numbers. This is the first explicit example of an infinite family of non-compact finite volume Coxeter polytopes in hyperbolic 4-space whose growth rates are of the conjectured arithmetic nature as well.

1. Introduction

Let $\mathbf{H}^d$ denote the hyperbolic d-space and $\overline{\mathbf{H}}^d$ its closure in $\mathbf{R}^d \cup \{\infty\}$. A d-dimensional convex polytope $P \subset \overline{\mathbf{H}}^d$ of finite volume is called a *Coxeter polytope* if all of its dihedral angles are of the form $\dfrac{\pi}{k}$ for an integer $k \geq 2$ or $k = \infty$, meaning that the intersection of the facets of P is a point on the boundary $\partial\mathbf{H}^d$. The set S of reflections with respect to the facets of P generates a discrete group Γ, called a (*d-dimensional*) *hyperbolic Coxeter group*, and the pair (Γ, S) is called the *Coxeter system* associated with P. If P is compact (resp. non-compact), the hyperbolic Coxeter group Γ is called *cocompact* (resp. *cofinite*). The *growth series* $f_S(t)$ of (Γ, S) and of P is the formal power series $1 + \sum_{l=1}^{\infty} a_l t^l$ where a_l is the number of elements of Γ whose word length with respect to S is equal to l. Then $\tau_\Gamma := \limsup_{l\to\infty} \sqrt[l]{a_l}$ is called the *growth rate* of (Γ, S) and of P.

It is known that the growth rate of a d-dimensional cofinite hyperbolic Coxeter group is a real algebraic integer strictly bigger than 1 [5]. Recall that a real algebraic number $\tau > 1$ is a Perron number if and only if all of its other

---

2010 *Mathematics Subject Classification*. Primary 20F55, Secondary 20F65.

Key words and phrases. Coxeter group; growth function; growth rate; Perron number.
Received September 3, 2018; revised November 19, 2018.

algebraic conjugates are strictly less than τ in absolute value. It is known that the growth rates of cofinite 2- and 3-dimensional hyperbolic Coxeter groups are always Perron numbers ([1], [3], [8], [10], [12], [13], [21], [22]). The growth rates of right-angled Coxeter groups are also Perron numbers [9].

The goal of this work is the study of the arithmetic nature of growth rates associated to 4-dimensional cofinite hyperbolic Coxeter groups. In the context of *compact* hyperbolic Coxeter 4-polytopes P, Kellerhals and Perren [7] showed that the growth rates of polytopes P with at most 6 facets are Perron numbers and formulated a conjecture for arbitrary dimensions d. Then, Umemoto [19] constructed an infinite sequence of compact hyperbolic Coxeter 4-polytopes as garlands based on a totally truncated 4-simplex. Inspired by [23], she was able to prove that their growth rates are 2-Salem numbers and therefore particular Perron numbers.

In this paper, we construct and study growth rates of infinitely many *non-compact* hyperbolic Coxeter 4-polytopes. More precisely, we first construct an infinite family of *ideal* and non-simple hyperbolic Coxeter 4-polytopes starting from a certain pyramid in $\mathbf{H}^4$, found by Tumarkin [18], whose apex at infinity has a (Euclidean) cubical structure (see Figure 4, Section 4.2). By exploiting results of Kronecker, we are able to prove that their growth rates are Perron numbers. In this way, we provide the first example of an infinite sequence of non-cocompact but cofinite 4-dimensional hyperbolic Coxeter groups satisfying the (generalized) conjecture of Kellerhals and Perren.

The paper is organized as follows. In Section 2, we provide the necessary background about the growth series $f_S(t)$, representing the rational growth function $\frac{p(t)}{q(t)}$, $p(t), q(t) \in \mathbf{Z}[t]$, of a d-dimensional hyperbolic Coxeter group Γ with natural generating system S. In Section 3, we explain in detail a method—going back to Sturm and Kronecker—which helps to analyze the root distribution of a real polynomial in the complex plane. Then, in Section 4, we construct an infinite sequence $\{P_n\}_{n\in\mathbf{N}}$ of ideal non-simple hyperbolic Coxeter 4-polytopes by glueing isometric copies of Tumarkin's Coxeter pyramid with 7 facets, and we provide a detailed analysis of the combinatorial and metrical structure of $\{P_n\}_{n\in\mathbf{N}}$. Finally, in Section 5, we apply the method described in Section 3 in order to analyze the root distribution of the denominator polynomials $D_n(t) \in \mathbf{Z}[t]$ of the growth functions $f_n(t)$ associated to the polyhedral sequence P_n. This allows us to prove that the growth rate τ_n of each P_n, $n \in \mathbf{N}$, is a Perron number (see Theorem 8). At the end, we attach an appendix listing the numerical data about the polynomials $D_n(t)$ which were found by means of the software package Mathematica.

2. Preliminaries

In this section, we introduce the relevant notation and review Solomon's and Steinberg's formulas in order to calculate the growth functions of hyperbolic Coxeter polytopes.

A *Coxeter system* (Γ, S) consists of a group Γ and a finite set of generators $S \subset \Gamma$, $S = \{s_i\}_{i=1}^{N}$, with relations $(s_i s_j)^{m_{ij}}$ for each i, j, where $m_{ii} = 1$ and $m_{ij} \geq 2$ or $m_{ij} = \infty$ for $i \neq j$. We call Γ a *Coxeter group*. For any subset $I \subset S$, we define Γ_I to be the subgroup of Γ generated by $\{s_i\}_{i \in I}$. Then (Γ_I, I) is a Coxeter system in its own right and Γ_I is called the *Coxeter subgroup* of Γ generated by I. The *Coxeter diagram* $X(\Gamma, S)$ of (Γ, S) is constructed as follows: Its vertex set is S, and if $m_{ij} \geq 3$, we join the pair of vertices s_i, s_j by an edge. For each edge, we label it with m_{ij} if $m_{ij} \geq 4$. Note that the Coxeter diagram of (Γ_I, I) for each subset $I \subset S$ is a subdiagram of $X(\Gamma, S)$. The *growth series* $f_S(t)$ of (Γ, S) is the formal power series $1 + \sum_{l=1}^{\infty} a_l t^l$ where a_l is the number of elements of Γ whose word length with respect to S is equal to l. Then $\tau_{(\Gamma,S)} = \limsup_{l \to \infty} \sqrt[l]{a_l}$ is called the *growth rate* of (Γ, S). A Coxeter system (Γ, S) is *irreducible* if the Coxeter diagram $X(\Gamma, S)$ is connected.

Next, we recall Solomon's formula and Steinberg's formula which enable us to express and calculate growth series of Coxeter systems as rational functions.

THEOREM 1 [16, Solomon's formula]. *The growth series $f_S(t)$ of an irreducible finite Coxeter system (Γ, S) is a polynomial of the form $f_S(t) = [m_1 + 1, m_2 + 1, \ldots, m_p + 1]$ where $[n] = 1 + t + \cdots + t^{n-1}$, $[m, n] = [m][n]$, etc., and where $\{m_1, m_2, \ldots, m_p\}$ is the set of exponents of (Γ, S).*

Irreducible finite Coxeter groups are well-known. Their exponents are given in Table 1 (see [6] for details).

Table 1. Exponents

Coxeter group	Exponents	growth series
A_n	$1, 2, \ldots, n$	$[2, 3, \ldots, n+1]$
B_n	$1, 3, \ldots, 2n-1$	$[2, 4, \ldots, 2n]$
D_n	$1, 3, \ldots, 2n-3, n-1$	$[2, 4, \ldots, 2n-2][n]$
E_6	$1, 4, 5, 7, 8, 11$	$[2, 5, 6, 8, 9, 12]$
E_7	$1, 5, 7, 9, 11, 13, 17$	$[2, 6, 8, 10, 12, 14, 18]$
E_8	$1, 7, 11, 13, 17, 19, 23, 29$	$[2, 8, 12, 14, 18, 20, 24, 30]$
F_4	$1, 5, 7, 11$	$[2, 6, 8, 12]$
H_3	$1, 5, 9$	$[2, 6, 10]$
H_4	$1, 11, 19, 29$	$[2, 12, 20, 30]$
$I_2(m)$	$1, m-1$	$[2, m]$

Theorem 2 [17, Steinberg's formula]. *Let* (Γ, S) *be an infinite Coxeter system. Set* $\mathscr{F} := \{I \subset S \mid \Gamma_I$ *is a finite Coxeter subgroup of* $\Gamma\}$. *Denote by* $f_I(t)$ *the growth series of* (Γ_I, I) *for each* $I \subset S$. *Then*

$$\frac{1}{f_S(t^{-1})} = \sum_{I \in \mathscr{F}} \frac{(-1)^{|I|}}{f_I(t)}.$$

By Theorem 1 and Theorem 2, the growth series $f_S(t)$ of (Γ, S) is represented by a rational function $\frac{p(t)}{q(t)}$ $(p, q \in \mathbf{Z}[t])$. The rational function $\frac{p(t)}{q(t)}$ is called the *growth function* of (Γ, S). The radius of convergence R of $f_S(t)$ is equal to the positive real root of $q(t)$ which has the smallest absolute value among all roots of $q(t)$.

In this paper, we are interested in Coxeter groups giving rise to discrete subgroups generated by reflections in the isometry group $\mathrm{Isom}(\mathbf{H}^d)$ of $\mathbf{H}^d$. The references here are [15] and [20]. More concretely, we represent hyperbolic d-space in the upper half-space model according to $\mathbf{H}^d = \{(x_1, \dots, x_d) \in \mathbf{R}^d \mid x_d > 0\}$ which is equipped with the metric $\frac{|dx|}{x_d}$. The boundary $\partial\mathbf{H}^d$ of $\mathbf{H}^d$ in the one-point compactification $\mathbf{R}^d \cup \{\infty\}$ of $\mathbf{R}^d$ is called the *boundary at infinity* of $\mathbf{H}^d$. We denote the closure of a subset $A \subset \mathbf{R}^d \cup \{\infty\}$ by $\bar{A}$. By identifying $\mathbf{R}^{d-1}$ with $\mathbf{R}^{d-1} \times \{0\}$ in $\mathbf{R}^d$, the boundary at infinity $\partial\mathbf{H}^d$ is equal to $\mathbf{R}^{d-1} \cup \{\infty\}$. A subset $H \subset \mathbf{H}^d$ is called a *hyperplane* of $\mathbf{H}^d$ if and only if it is either a Euclidean hemisphere or a half-plane in $\mathbf{H}^d$ orthogonal to $\mathbf{R}^{d-1}$.

A non-empty subset $P \subset \overline{\mathbf{H}}^d$ is called a *d-dimensional hyperbolic polytope* if P can be written as the intersection of finitely many closed half-spaces. This means that $P = \bigcap H_i^-$, where H_i^- is the closed half-space of $\mathbf{H}^d$ bounded by the hyperplane H_i with normal vector u_i pointing outwards with respect to P. Suppose that $H_i \cap H_j \neq \emptyset$ in $\mathbf{H}^d$. Then, the *dihedral angle* between H_i and H_j is given as follows: Choose a point $x \in H_i \cap H_j$ and consider their outer normal vectors u_i and u_j. The dihedral angle between H_i and H_j is defined as the number $\theta \in [0, \pi]$ satisfying $\cos\theta = -(u_i, u_j)$ where $(\cdot, \cdot)$ denotes the Euclidean inner product on $\mathbf{R}^d$ at x. If $\overline{H_i} \cap \overline{H_j} \in \overline{\mathbf{H}}^d$ is a point on $\partial\mathbf{H}^d$, then the dihedral angle between H_i and H_j is defined to be zero.

A hyperbolic polytope $P \subset \overline{\mathbf{H}}^d$ of finite volume is called a *hyperbolic Coxeter polytope* if all of its dihedral angles have the form $\frac{\pi}{k}$ for an integer $k \geq 2$ or $k = \infty$ if the intersection of respective bounding hyperplanes is a point on $\partial\mathbf{H}^d$. Notice that a hyperbolic polytope in $\overline{\mathbf{H}}^d$ is of finite volume if and only if it is the convex hull of finitely many points in $\overline{\mathbf{H}}^d$. If $P \subset \overline{\mathbf{H}}^d$ is a hyperbolic Coxeter polytope, the set S of all reflections with respect to the facets of P generates a discrete group Γ in $\mathrm{Isom}(\mathbf{H}^d)$. It is easy to see that (Γ, S) is a

Coxeter system so that Γ is a Coxeter group. We call Γ a *d-dimensional hyperbolic Coxeter group*. The pair (Γ, S) is called the *Coxeter system associated to P*. In the sequel, we call the growth function and the growth rate of the Coxeter system (Γ, S) associated to P the *growth function of P* and the *growth rate of P*. The growth function and the growth rate of P are denoted by $f_P(t)$ and τ_P, respectively.

Let $P = \bigcap_{i=1}^N H_i^-$ be a hyperbolic Coxeter polytope. For every pair of hyperplanes H_i and H_j, define

$$c_{ij} = \begin{cases} 1 & \text{if } i = j, \\ -\cos \dfrac{\pi}{m_{ij}} & \text{if they intersect at the dihedral angle } \dfrac{\pi}{m_{ij}}, \\ -1 & \text{if its intersection is a point on } \partial \mathbf{H}^d, \\ -\cosh d(H_i, H_j) & \text{if they do not intersect,} \end{cases}$$

where $d(H_i, H_j)$ is the hyperbolic distance between them. The $N \times N$ symmetric matrix $M(P) = (c_{ij})$ is called the *Gram matrix of P*. The *Coxeter scheme $X(P)$ of P* is defined as follows: Its vertex set is $\{H_1, \dots, H_N\}$, and for $m_{ij} \geq 3$, we join the pair of vertices H_i, H_j by an edge. For each edge, we label it with m_{ij} if $m_{ij} \geq 4$. Two vertices are joined by a dotted edge labeled with the hyperbolic distance between corresponding hyperplanes if H_i and H_j do not intersect. A subscheme of $X(P)$ is called *elliptic* (resp. *parabolic*) if the corresponding submatrix of $M(P)$ is positive definite (resp. positive semi-definite of rank $d-1$). Note that elliptic subschemes *of order k*, that is, with k vertices, correspond to finite Coxeter systems (Γ, S) with $|S| = k$. In the hyperbolic context, they can be characterized as follows.

Theorem 3 [20, Theorem 2.2, p. 109 and Theorem 2.5, p. 110]. *Given a hyperbolic Coxeter polytope P, the k-dimensional faces (resp. vertices at infinity) of P correspond to the order $n-k$ elliptic (resp. parabolic) subschemes of the Coxeter scheme $X(P)$ of P.*

3. Describing the root distribution of a real polynomial

In this section, we review Sturm's theorem and Kronecker's theorem. Sturm's theorem allows one to describe the distribution of the real roots of a real polynomial, while Kronecker's theorem is about counting the roots of a real polynomial contained in a closed disk of radius r centered at the origin 0 in the complex plane $\mathbf{C}$. For references, see [2], [11] and [14].

3.1. Sturm's theorem. Let f and g be real polynomials. We may assume that $\deg f \geq \deg g$. By the Euclidean algorithm, there are polynomials $f_2, \dots, f_r$ such that

$$f = q_1 g - f_2, \quad \deg g > \deg f_2.$$
$$g = q_2 f_2 - f_3, \quad \deg f_2 > \deg f_3.$$
$$f_2 = q_3 f_3 - f_4, \quad \deg f_3 > \deg f_4.$$
$$\vdots$$
$$f_{r-2} = q_{r-1} f_{r-1} - f_r, \quad \deg f_{r-1} > \deg f_r.$$
$$f_{r-1} = q_r f_r.$$

The finite sequence $f_0 := f, f_1 := g, f_2, \dots, f_r$ of real polynomials is called the *Sturm sequence* $S(f,g)$ *of* f *and* g. Note that f_r is the greatest common divisor of f and g. For any $t_0 \in \mathbf{R}$, the number of sign changes in $S(f,g)$ at t_0 is denoted by $w(t_0)$, that is, $w(t_0)$ is the number of sign changes in the sequence $f(t_0), g(t_0), f_2(t_0), \dots, f_r(t_0)$ ignoring zeros.

Example 1. Let $f(z) := z^5 - 3z - 1$ and $g(z) := f'(z) = 5z^4 - 3$. Then, $S(f,g)$ can be calculated as follows:

$$f(z) = z^5 - 3z - 1.$$
$$g(z) = 5z^4 - 3.$$
$$f_2(z) = 12z + 5.$$
$$f_3(z) = 1.$$

We consider the number of sign changes in the Sturm sequence $S(f,g)$ at $t_0 = -2$. We have $f(-2) = -27$, $g(-2) = 77$, $f_2(-2) = -19$, $f_3(-2) = 1$, so that $w(-2)$ is equal to 3.

Theorem 4 [2, Theorem 8.8.15, Sturm's theorem]. *Let* f *be a real polynomial and* $S(f,f') = \{f_0, f_1, \dots, f_r\}$. *Suppose that* $a, b \in \mathbf{R}$, $a < b$, *are not roots of* f. *Then the number of distinct real roots of* f *in the closed interval* $[a,b]$ *is equal to* $w(a) - w(b)$.

From now on, we assume that the real polynomials f and g have no common roots. For each real root t_0 of f, the number of sign changes in $S(f,g)$ satisfies one of the following three conditions:

(i) The number of sign changes in $S(f,g)$ decreases by 1 when t passes through t_0.

(ii) The number of sign changes in $S(f,g)$ increases by 1 when t passes through t_0.

(iii) The number of sign changes in $S(f,g)$ does not vary when t passes through t_0.

We assign the number $\varepsilon_{t_0} = 1, -1$ and 0 to each root t_0 of f when the number of sign changes of $f(t)$, $g(t)$ satisfies the condition (i), (ii) and (iii), respectively. The following well-known theorem is proved analogously to Sturm's theorem.

Theorem 5. *Suppose that the real numbers a and b, $a < b$, are not roots of f. Then, the following identity holds for $S(f, g)$.*

$$\sum_{t_0 \in [a,b]: f(t_0)=0} \varepsilon_{t_0} = w(a) - w(b).$$

3.2. Separation of complex roots. We use the following notation:

- $\mathbf{C}_z$ and $\mathbf{C}_\varsigma$ denote respectively the complex planes with coordinates $z = x + iy$ and $\varsigma = u + iv$.
- $S_r \subset \mathbf{C}_z$ is a circle of radius $r > 0$ centered at the origin $0 \in \mathbf{C}_z$.
- $B_r \subset \mathbf{C}_z$ is an open disk of radius $r > 0$ centered at 0.
- A parametrization for S_r is given by

$$z(t) = r\frac{t^2-1}{t^2+1} - ir\frac{2t}{t^2+1}, \quad t \in \mathbf{R}.$$

- $f(z)$ is a real polynomial of a complex variable z.
- Expanding $f(z(t))$ yields the representation

$$f(z(t)) = \frac{\varphi_r(t) + i\psi_r(t)}{(t^2+1)^{\deg f}} \quad \text{on } S_r,$$

where $\varphi_r(t)$ and $\psi_r(t)$ are real polynomials of the real variable t.

Next, we explain Kronecker's theorem.

Lemma 1. *Suppose that $f(z)$ has no roots on S_r. Given $M > 0$ such that the closed interval $[-M, M]$ contains all real roots of φ_r, the following identity holds for $S(\varphi_r, \psi_r)$.*

$$\sum_{t_0 \in [-M,M]: \varphi_r(t_0)=0} \varepsilon_{t_0} = w(-M) - w(M).$$

Proof. The assumption that $f(z)$ has no roots on S_r implies that the polynomials $\varphi_r(t)$ and $\psi_r(t)$ do not have common real roots. Now, apply Theorem 4 to $\varphi_r(t)$ and $\psi_r(t)$, and the assertion follows. □

By considering $f(z)$ as a holomorphic function from $\mathbf{C}_z$ to $\mathbf{C}_\varsigma$, we parametrise the closed curve $f(S_r)$ according to $\varsigma(t) = \dfrac{\varphi_r(t)}{(t^2+1)^{\deg f}} + i\dfrac{\psi_r(t)}{(t^2+1)^{\deg f}}$ for $t \in \mathbf{R}$. In order to calculate the winding number of $f(S_r)$, we divide $f(S_r)$ into oriented closed curves $C_1, \dots, C_m$ as follows. Trace $f(S_r)$ by starting from the initial point $f(r) = \lim_{t \to -\infty} \varsigma(t)$, and if the curve $f(S_r)$ crosses the v-axis in $\mathbf{C}_\varsigma$ (at least) twice, we mark the (first) two crossing points by α_1 and α_2 on the v-axis. and then go back to the initial point $f(r)$ along the straight line from the point α_2 to the initial point $f(r)$. This locus defines the oriented closed curve C_1 (see the top right part of Fig. 1). Next, we go back to $f(S_r)$ along the straight line from

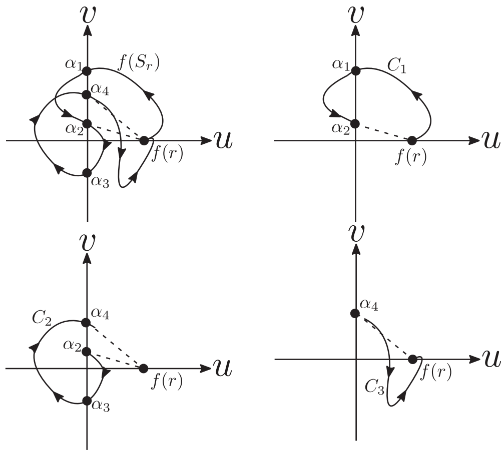

FIGURE 1. Subdivision of the closed curve $f(S_r)$

$f(r)$ to α_2 and repeat the procedure for the next pair of crossing points α_3 and α_4 which provides an oriented closed curve C_2 from $f(r)$ via a straight line to α_2, the part of $f(S_r)$ from α_2 to α_4 and then back via a straight line to $f(r)$. By repeating this procedure, the closed curve $f(S_r)$ gets subdivided and yields oriented closed curves $C_1, \dots, C_m$ (see Fig. 1). Let us add that the final intersection point α_f of $f(S_r)$ with the v-axis gives rise to the oriented closed C_m given by the straight line from $f(r)$ to α_f combined with the part of $f(S_r)$ from α_f back to $f(r)$.

Given such a subdivision of $f(S_r)$, the winding number of $f(S_r)$ equals the sum of the winding numbers of oriented closed curves $C_1, \dots, C_m$. In order to calculate the winding number of each curve C_i, we assign the number $\chi_{\alpha_k} = 1$ (resp. $\chi_{\alpha_k} = -1$) to a crossing point $\alpha_k \in C_i$ on the v-axis if the (angular) argument in the parametrization of C_i is increasing (resp. decreasing) in the counterclockwise sense around the point α_k (see Fig. 2). In this way, the winding number of C_i is equal to the sum of $\frac{1}{2}\chi_\alpha$ at each of its crossing points α. Note that if a

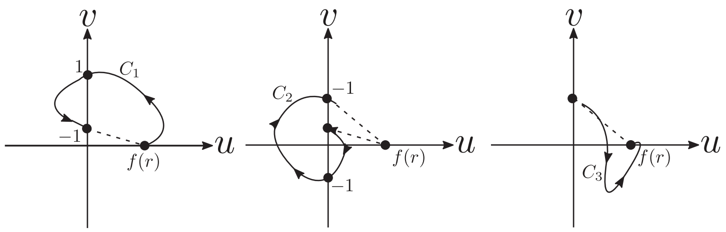

FIGURE 2. Assigning the numbers χ_α to crossing points α

component C_i has no crossing points of v-axis, then the winding number of C_i equals 0. For example, the winding number of C_1, C_2 and C_3 in Fig. 2 is equal to 0, -1 and 0, respectively. This observation shows that the winding number of $f(S_r)$ equals the sum of numbers $\frac{1}{2}\chi_\alpha$ for each crossing point α of v-axis and $f(S_r)$.

Let us now consider the Sturm sequence of polynomials $\varphi_r(t)$ and $\psi_r(t)$. Every crossing point of curve $f(S_r)$ corresponds to a root of $\varphi_r(t)$. For any root $t_0 \in \mathbf{R}$ of $\varphi_r(t)$, the argument of $f(S_r)$ is increasing (resp. decreasing) if $\varepsilon_{t_0} = -1$ (resp. $\varepsilon_{t_0} = 1$). This observation, together with Theorem 4 and the argument principle, give the following identities.

$$\begin{aligned}\#\{z \in B_r \mid z \text{ is a root of } f(z)\} &= \text{the winding number of } f(S_r) \\ &= \frac{1}{2} \sum_{\alpha_k:\ \text{a mark on } f(S_r)} \chi_{\alpha_k} \\ &= \frac{1}{2} \sum_{t_0:\varphi_r(t_0)=0} (-\varepsilon_{t_0}).\end{aligned}$$

By Lemma 1, one can deduce Kronecker's theorem as follows.

THEOREM 6 [14, Theorem 1.4.6, Kronecker's theorem]. *Suppose that $f(z)$ has no roots on S_r. Then, the number of roots of f contained in B_r equals to $\dfrac{w(M) - w(-M)}{2}$, where $M > 0$ is a real number such that $[-M, M]$ contains all roots of $\varphi_r(t)$.*

If we substitute $z(t) = r\dfrac{t-i}{t+i}$ in $f(z)$, then $f(z(t))$ can be rewritten according to

$$f(z(t)) = \frac{\Phi(t) + i\Psi(t)}{(t+i)^{\deg f}}.$$

Since $\dfrac{1}{2\pi}\int_{f(S_r)} d\log w = \dfrac{1}{2\pi}\int_{f(S_r)} d\arg w$ (see [4]), the winding number of $f(S_r)$ equals $\dfrac{1}{2\pi}\int_{-\infty}^{\infty} \arg\{\Phi(t) + i\Psi(t)\}\,dt - \dfrac{1}{2\pi}\int_{-\infty}^{\infty} \arg(t+i)^{\deg f}\,dt$. For brevity, we denote the quantities $\dfrac{1}{2\pi}\int_{-\infty}^{\infty} \arg\{\Phi(t) + i\Psi(t)\}\,dt$ and $\dfrac{1}{2\pi}\int_{-\infty}^{\infty} \arg(t+i)^{\deg f}\,dt$ by $\Theta(\Phi(t) + i\Psi(t))$ and $\Theta((t+i)^{\deg f})$. Then, $\Theta(\Phi(t) + i\Psi(t))$ and $\Theta((t+i)^{\deg f})$ measure the extent of argument increase of the curves $\Phi(t) + i\Psi(t)$ and $(t+i)^{\deg f}$, $t \in \mathbf{R}$, respectively (see [4] for details). Applying the previous arguments to the curve $\Phi(t) + i\Psi(t)$, $t \in \mathbf{R}$, we obtain the identification

$$\Theta(\Phi(\mathbf{R}) + i\Psi(\mathbf{R})) = \frac{w(M) - w(-M)}{2}.$$

By substituting $t = \tan\theta$, a calculation yields

$$\Theta((\mathbf{R}+i)^{\deg f}) = -\frac{\deg f}{2}.$$

Therefore, we obtain the following corollary of Kronecker's theorem.

COROLLARY 1. *Suppose that $f(z)$ has no roots on S_r. Let $w(t)$ denote the number of sign changes in the Sturm sequence of $\Phi(t)$ and $\Psi(t)$. Then, the number of roots of $f(z)$ contained in B_r equals to* $\dfrac{w(M) - w(-M) + \deg f}{2}$.

For any real polynomial f, the sign of $f(t)$ for sufficiently large (resp. small) $t \in \mathbf{R}$ is determined by its leading coefficient (resp. multiplied by $(-1)^{\deg f}$). Therefore, in order to determine $w(M)$, we only have to consider the leading coefficients of the polynomials in the Sturm sequence $S(\Phi, \Psi)$ of $\Phi(t)$ and $\Psi(t)$. For the rest of the paper, $w(\infty)$ (resp. $w(-\infty)$) denotes the number of sign changes of the leading coefficients (resp. multiplied by $(-1)^{\deg f_i}$) of $S(\Phi, \Psi)$.

3.3. A method for describing the root distribution of a real polynomial. Suppose $f(z)$ is a real polynomial. Then, we can describe its roots as follows.

In order to count the number of the real roots of f contained in the closed interval $[a, b]$, we proceed as follows.

1. Check that a and b are not roots of f.
2. Calculate the Sturm sequence $S(f, f')$ of $f(t)$ and $f'(t)$.
3. By Sturm's theorem, $w(a) - w(b)$ is equal to the number of real roots of f contained in $[a, b]$.

In order to count the number of roots of f contained in B_r, one performs the following steps.

1. Calculate the two real polynomials $\Phi(t)$ and $\Psi(t)$ by substituting $z(t) = r\dfrac{t-i}{t+i}$ into $f(z)$.
2. Check that $f(z)$ has no roots on S_r. To this end, recall that if the resultant of $\Phi(t)$ and $\Psi(t)$ is not 0, then $f(z)$ has no roots on S_r.
3. Calculate the Sturm sequence $S(\Phi, \Psi)$ of $\Phi(t)$ and $\Psi(t)$.
4. By Corollary 1 and the definition of $w(\infty)$ and $w(-\infty)$, the number of roots of f contained in B_r is equal to $\dfrac{w(\infty) - w(-\infty) + \deg f}{2}$.

4. The construction of an infinite sequence of ideal non-simple hyperbolic Coxeter polytopes

We construct an infinite sequence $\{P_n\}_{n \in \mathbf{N}}$ of non-simple ideal hyperbolic Coxeter 4-polytopes by glueing copies of certain ideal hyperbolic Coxeter

4-pyramid along their isometric facets. First, we consider the vertical projection p_∞ from ∞ to $\mathbf{R}^3$ and describe a hyperbolic 4-polytope by means of its projective image. In the sequel, we call polygonal faces of a 4-polytope *faces* for brevity.

4.1. The vertical projection from ∞. A *horosphere* $\Sigma = \Sigma_u$ *based at a point at infinity* $u \in \partial \mathbf{H}^d$ is defined to be a 3-dimensional Euclidean sphere in $\mathbf{H}^4$ tangent to $\mathbf{R}^3$ at u (resp. a Euclidean hyperplane parallel to $\mathbf{R}^3$) if u is situated on $\mathbf{R}^3$ (resp. $u = \infty$). The restriction of the hyperbolic metric to the horosphere Σ turns Σ into a Euclidean 3-space.

Lemma 2 [15, Theorem 6.4.5]. *Suppose that $P = \bigcap_{i=1}^m H_i^-$ is a non-compact hyperbolic 4-polytope of finite volume and u is a vertex at infinity of P. Let Σ be a horosphere based at u such that Σ intersects with P only at the bounding hyperplanes incident to u. Then, $L(u) := P \cap \Sigma$ has the following properties.*

- *$L(u)$ is a 3-dimensional Euclidean polytope in Σ.*
- *For any bounding hyperplane H_i incident to u, $H_i \cap L(u)$ is a bounding hyperplane of $L(u)$ in Σ.*
- *If two facets $F_i := H_i \cap P$ and $F_j := H_j \cap P$ form a face of P, then the intersection of $F_i \cap L(u)$ and $F_j \cap L(u)$ is an edge of $L(u)$ and the dihedral angle $\angle F_i \cap F_j$ is equal to the dihedral angle $\angle (F_i \cap L(u)) \cap (F_j \cap L(u))$.*

Consider *the vertical projection from ∞* denoted by

$$p_\infty : \mathbf{H}^4 \to \mathbf{R}^3; \quad (x, y, z, t) \mapsto (x, y, z).$$

Let $P = \bigcap_{i=1}^m H_i^-$ be a non-compact hyperbolic 4-polytope of finite volume and u be a vertex at infinity of P. By using the hyperbolic isometries induced by the translation of $\mathbf{R}^3$ which maps u to 0 and the inversion with respect to the unit sphere in $\mathbf{R}^4$, we may assume that u is ∞. If a hyperplane H_i is incident to (resp. not incident to) ∞, then H_i is a Euclidean hyperplane (resp. hemisphere) in $\mathbf{H}^4$ orthogonal to $\mathbf{R}^3$. Note that in our setting any closed half-space H_i^- contains ∞. Since the vertical projection p_∞ maps any horosphere Σ based at ∞ conformally onto $\mathbf{R}^3$, by using Lemma 2, we can treat dihedral angles between two bounding hyperplanes of P incident to ∞ as the corresponding dihedral angles in the 3-dimensional Euclidean polytope $p_\infty(L(\infty))$. Suppose that the bounding hyperplanes H_i and H_j of P are not incident to ∞. By choosing a point in $H_i \cap H_j \cap \mathbf{R}^3$ and considering the outer normal vectors u_i and u_j, the dihedral angle $\angle H_i \cap H_j$ in P is given by $\arccos(-(u_i, u_j))$.

4.2. The ideal hyperbolic Coxeter pyramid P_1. In [18], Tumarkin classified all hyperbolic Coxeter 4-pyramids whose apex at infinity has a cubical structure. In particular, there exists an ideal hyperbolic Coxeter 4-pyramid P_1 with Coxeter scheme shown in Figure 4.

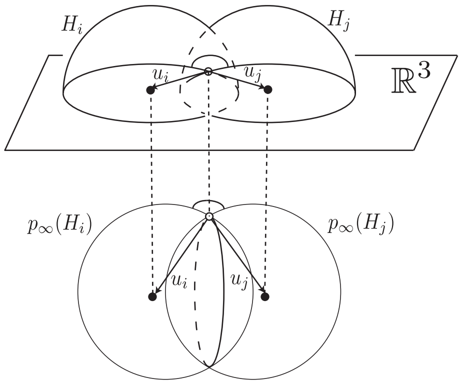

FIGURE 3. The dihedral angle in $\mathbf{R}^3$

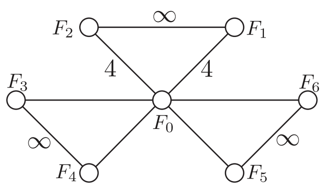

FIGURE 4. The Coxeter scheme $X(P_1)$

In the sequel, we use the following notations.

- The non-simple vertex of P_1 is denoted by u.
- F_0 denotes the unique cubical facet of P_1.
- The pyramidal facets of P_1 are denoted by $F_1, \ldots, F_6$. The facets have the property that F_i and F_{i+1} $(i = 1, 3, 5)$ meet at the non-simple vertex u of P_1 and the dihedral angle formed by F_i and F_0 is equal to $\dfrac{\pi}{4}$ for $i = 1, 2$.
- If the intersection of facets F_i and F_j is a face of P_1, we denote it by f_{ij}. In particular, f_{ij} is the ridge of dihedral angle $\angle F_i \cap F_j$.
- The hyperplane carrying F_i is denoted by H_i.

Since the vertex link of u is a Euclidean right-angled cube given by $\tilde{A}_1 \times \tilde{A}_1 \times \tilde{A}_1$, and by using suitable isometries of $\mathbf{H}^4$, P_1 can be normalized as follows.

- The vertex u is ∞.
- The hyperplane H_0 is the unit hemisphere centered at origin.
- The hyperplanes H_1 and H_2 are orthogonal to the x-axis.
- The hyperplanes H_3 and H_4 are orthogonal to the y-axis.
- The hyperplanes H_5 and H_6 are orthogonal to the z-axis.

Under this normalization for P_1, we can depict $p_\infty(P_1)$ according to Figure 5. The coordinates of eight vertices A, B, C, D, E, F, G and H are

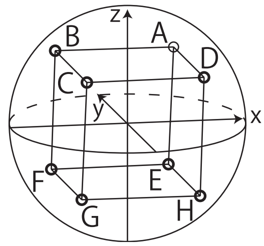

FIGURE 5. The projective image $p_\infty(P_1)$ of P_1 in $\mathbf{R}^3$

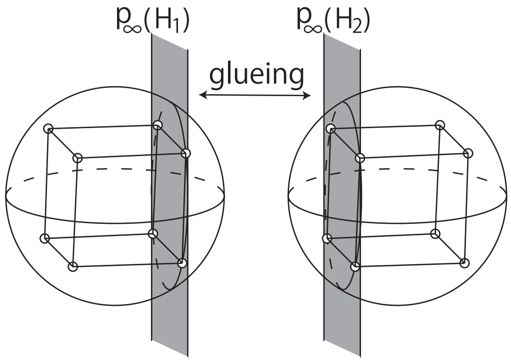

FIGURE 6. The projective images of P_1 and P_1'

$$A=\left(\frac{1}{\sqrt{2}},\frac{1}{2},\frac{1}{2}\right)\quad B=\left(-\frac{1}{\sqrt{2}},\frac{1}{2},\frac{1}{2}\right)\quad C=\left(-\frac{1}{\sqrt{2}},-\frac{1}{2},\frac{1}{2}\right)$$
$$D=\left(\frac{1}{\sqrt{2}},-\frac{1}{2},\frac{1}{2}\right)\quad E=\left(\frac{1}{\sqrt{2}},\frac{1}{2},-\frac{1}{2}\right)\quad F=\left(-\frac{1}{\sqrt{2}},\frac{1}{2},-\frac{1}{2}\right)$$
$$G=\left(-\frac{1}{\sqrt{2}},-\frac{1}{2},-\frac{1}{2}\right)\quad H=\left(\frac{1}{\sqrt{2}},-\frac{1}{2},-\frac{1}{2}\right).$$

In Figure 5, the hyperplanes carrying the quadrangular faces ADHE, ABFE and ABCD are $p_\infty(H_1)$, $p_\infty(H_3)$ and $p_\infty(H_5)$. Now, we take a copy of P_1, denoted by P_1', such that the facet F_k' of P_1' is isometric to the facet F_k of P_1 for $k=0,\dots,6$. Glue the two 4-pyramids P_1 and P_1' along the facet F_1 of P_1 and the facet F_2' of P_1' to obtain a new polytope P_2.

The projective image of P_2 is depicted in Figure 7. By the glueing procedure, the facets F_1 of P_1 and F_2' of P_1' do not appear in P_2. Since the hyperplanes $p_\infty(H_3)$, $p_\infty(H_4)$, $p_\infty(H_5)$ and $p_\infty(H_6)$ of P_1 and P_1' coincide with each other, the faces f_{13}, f_{14}, f_{15}, f_{16} in P_1 and f_{23}, f_{24}, f_{25}, f_{26} in P_1' do not appear in P_2 as well. On the other hand, P_2 has some new faces; one is the quadrangular

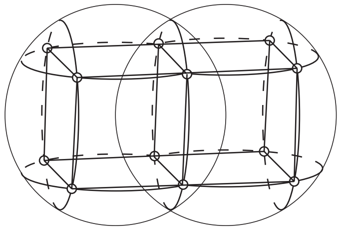

FIGURE 7. The projective image of the resulting 4-polytope P_2.

face coming from the cubical facet F_0 in P_1 and P_1', and the other new faces are composed by the unions of f_{34}, f_{45}, f_{56} and f_{63} in $P_1 \cup P_1'$. Since the pyramidal facets F_2 in P_1 and F_1' in P_1' do not contribute to the glueing procedure, P_2 has the two facets F_1 and F_2 in its boundary.

In summary, we obtain the following combinatorial data for P_2.

- P_2 has 8 facets; 2 cubical facets, 2 pyramidal facets and 4 facets with 6 faces.
- P_2 has 23 faces; (i) 8 triangular faces come from F_2 of P_1 and F_1' of P_1', (ii) 10 quadrangular faces come from F_0 in P_1 and P_1', (iii) only one quadrangular face comes from the intersection of F_1 in P_1 and F_2' in P_1', (iv) 4 quadrangular faces come from the union of f_{34}, f_{45}, f_{56} and f_{63} of P_1 and P_1'.
- P_2 has 28 edges.
- P_2 has 13 ideal vertices; only the vertex ∞ is non-simple.

Since the two pyramidal facets of P_2 are isometric to the pyramidal facets F_1 and F_2 of P_1, we can repeat this procedure by glueing P_1 and P_2 along their pyramidal facets, and the resulting 4-polytope is denoted by P_3. By induction, glueing a copy of P_1 to P_{n-1} gives rise to a new polytope denoted by P_n. In fact, the ideal hyperbolic 4-polytope P_n is obtained by glueing n copies of P_1 along the isometric facets F_1 and F_2.

4.3. The combinatorial structure of P_n.

LEMMA 3. *P_n has the following combinatorial data.*

(Facets) $(n+6)$ *facets*; *n cubical facets*, 2 *pyramidal facets and the other* 4 *facets have* $(n+4)$*-gonal faces.*

(Faces) $(5n+13)$ *faces*; 8 *triangular faces*, $5n+1$ *quadrilateral faces and* 4 $(n+2)$*-gonal faces.*

(Edges) $(8n+12)$ *edges.*

(Vertices) $(4n+5)$ *vertices*; $4n+4$ *simple vertices and only one non-simple vertex.*

Proof. It suffices to consider $p_\infty(P_n)$. Indeed, the projective image P_n consists of n right-angled cubes inscribed in closed balls of radius 1 (see Fig. 8). □

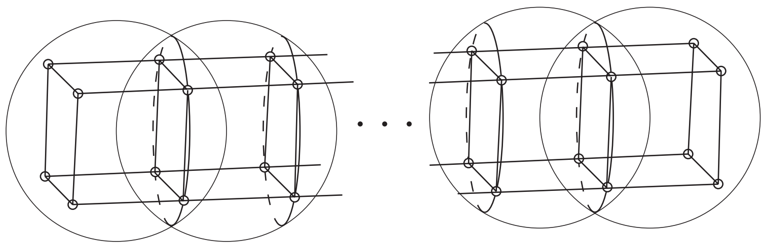

FIGURE 8. The projective image of P_n

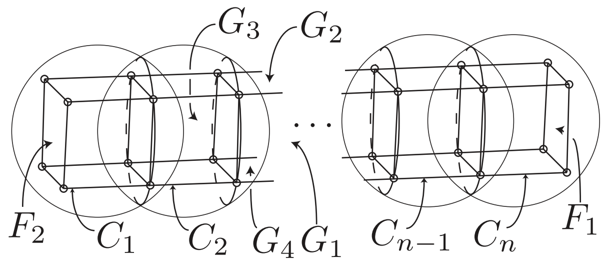

FIGURE 9. The front, top, back, and bottom planes are labeled by G_1, G_2, G_3, and G_4, respectively, following the notations for P_n.

We use the following notation and terminology to describe P_n.

- The 2 pyramidal facets of P_n are denoted by F_1 and F_2.
- The n cubical facets of P_n are denoted by $C_1, \ldots, C_n$. Moreover, we suppose that $C_1 \cap F_1$, $C_n \cap F_2$ and $C_i \cap C_{i+1}$ are the quadrilateral faces.
- The remaining facets of P_n are denoted by G_1, G_2, G_3, G_4. Moreover, we suppose that $G_i \cap G_{i+1}$ ($i \bmod 4$) is a $(n+2)$-gonal face.
- X_n denotes the Coxeter scheme of P_n.
- If a face of P_n has the dihedral angle $\frac{\pi}{m}$, we call it a $\frac{\pi}{m}$-*face.*

Let us determine the elliptic and parabolic subschemes of X_n.

(1) By Lemma 3, X_n has $n+6$ vertices.

(2) Since each quadrilateral face $C_i \cap C_{i+1}$ is the intersection of glueing facets, its dihedral angle $\angle C_i \cap C_{i+1}$ is equal to $\frac{\pi}{2}$. If we glue P_{n-1} and P_1 along their isometric pyramidal facets, then all faces of P_{n-1} and P_1 which are not incident to the glueing facets are invariant. Therefore, we have the following situation.

- The triangular faces $F_i \cap G_j$ are $\frac{\pi}{2}$-faces.
- The $(n+2)$-gonal faces $G_i \cap G_{i+1}$ are $\frac{\pi}{2}$-faces.

- The quadrilateral faces $G_i \cap C_j$ are $\frac{\pi}{3}$-faces.
- The quadrilateral faces $C_1 \cap F_1$ and $C_n \cap F_2$ are $\frac{\pi}{4}$-faces.

(3) Each edge of P_n is expressed as the intersection of precisely three facets.
- If an edge is the intersection $F_i \cap G_j \cap G_{j+1}$, it corresponds to the elliptic subscheme $A_1 \times A_1 \times A_1$ of X_n.
- If an edge is the intersection $F_1 \cap G_i \cap C_1$ or $F_2 \cap G_i \cap C_n$, it corresponds to the elliptic subscheme B_3 of X_n.
- If an edge is the intersection $G_i \cap G_{i+1} \cap C_j$, it corresponds to the elliptic subscheme A_3 of X_n.
- If an edge is the intersection $G_i \cap C_j \cap C_{j+1}$, it corresponds to the elliptic subscheme A_3 of X_n.

(4) Each vertex corresponds to a parabolic subscheme of X_n.
- If a vertex is the intersection $F_1 \cap G_i \cap G_{i+1} \cap C_1$ or $F_2 \cap G_i \cap G_{i+1} \cap C_n$, then it corresponds to the parabolic subscheme $\tilde{B}_3$ of X_n.
- If a vertex is the intersection $G_i \cap G_{i+1} \cap C_j \cap C_{j+1}$, then it corresponds to the parabolic subscheme $\tilde{A}_3$ of X_n.
- The non-simple vertex corresponds to the parabolic subscheme $\tilde{A}_1 \times \tilde{A}_1 \times \tilde{A}_1$ of X_n.

5. The growth function of P_n

By implementing the combinatorial data of P_n into Steinberg's formula (see Theorem 2), the growth function $f_n(t)$ of P_n can be calculated as follows.

$$\frac{1}{f_n(t^{-1})} = 1 - \frac{n+6}{[2]} + \frac{n+11}{[2,2]} + \frac{4n}{[2,3]} + \frac{2}{[2,4]} - \frac{8}{[2,2,2]} - \frac{8}{[2,4,6]} - \frac{8n-4}{[2,3,4]}.$$

By using Mathematica, the growth function $f_n(t)$, written as

$$f_n(t^{-1}) =: \frac{N_n(t)}{D_n(t)},$$

can be expressed according to

$$\begin{aligned} N_n(t) &= (t+1)^3(t^2+1)(t^2-t+1)(t^2+t+1), \\ D_n(t) &= t^9 - (n+3)t^8 - (n-4)t^7 + (2n-8)t^6 + (2n+8)t^5 + (2n-8)t^4 \\ &\quad - (2n-11)t^3 + (3n-5)t^2 + (3n+4)t - 4(n+1). \end{aligned}$$

LEMMA 4. *All the roots of $D_n(t)$ are simple.*

Proof. We show that the resultant $R(D_n(t), D_n'(t))$ of $D_n(t)$ and $D_n'(t)$ is not equal to 0 for any $n \in \mathbf{N}$. By using Mathematica, we can calculate it as follows:

$$
\begin{aligned}
R(D_n(t), D_n'(t)) = {} & 9367548196608n^{16} - 84315693201408n^{15} - 3211145218356480n^{14} \\
& - 13452086684085248n^{13} - 76883986729280512n^{12} \\
& - 221310749589989376n^{11} - 369276695931527424n^{10} \\
& - 436823682353681408n^{9} - 375744535536699392n^{8} \\
& - 227155659791212544n^{7} - 100271146222672128n^{6} \\
& - 28147372028425216n^{5} - 2791806794781440n^{4} \\
& - 1194005028478976n^{3} - 23952968404992n^{2} - 2787725279232n.
\end{aligned}
$$

By using Descartes' rule [14, Corollary 1, p. 28], $R(D_n(t), D_n'(t))$ has at most one positive real root as a real polynomial with respect to the index n. We can check the following equalities by using Mathematica.

$$
\begin{aligned}
R(D_{25}(t), D_{25}'(t)) &= -523676408952854830616241986910080 0, \\
R(D_{26}(t), D_{26}'(t)) &= 18356309345841539117459400503775232.
\end{aligned}
$$

Hence, $R(D_n(t), D_n'(t)) \neq 0$ for any $n \in \mathbf{N}$. □

5.1. The distribution of the real roots of $D_n(t)$.

LEMMA 5. *Let $w(t)$ be the number of sign changes in the Sturm sequence $S(D_n, D_n')$. Then,*

$$
w(0) = \begin{cases} 6 & (1 \leq n \leq 25) \\ 5 & (26 \leq n) \end{cases} \quad \text{and} \quad w(\infty) = \begin{cases} 3 & (1 \leq n \leq 25) \\ 2 & (26 \leq n) \end{cases}.
$$

Moreover, by Sturm's theorem, the number of positive real roots of $D_n(t)$ is equal to 3 for any $n \in \mathbf{N}$.

Proof. The equality $D_n(0) = -4(n+1)$ implies that 0 is not a root of $D_n(t)$ for any $n \in \mathbf{N}$. By using Mathematica, the Sturm sequence $S(D_n, D_n')$ can be calculated easily (see Appendix). Let us write $S(D_n, D_n') =: \{d_0, \dots, d_9\}$, and denote the i-th coefficient of $d_k(t) \in \mathbf{Q}[t]$ as $a_i^{(k)}$, that is,

$$
(*) \qquad d_k(t) = \sum_{i=0}^{9-k} a_i^{(k)} t^i.
$$

Then, $w(0)$ (resp. $w(\infty)$) is equal to the number of sign changes in the sequence $a_0^{(0)}, \dots, a_0^{(9)}$ (resp. $a_9^{(0)}, a_8^{(1)}, \dots, a_1^{(8)}, a_0^{(9)}$). The sign of each coefficient $a_i^{(k)}$ depends on $n \in \mathbf{N}$. Let us investigate these signs. For example, let us check the sign of $a_0^{(5)}$. The sign of $a_0^{(5)}$ depends on the following factor polynomial $p(n)$ (see Appendix):

$$p(n) = 13008n^8 + 20600n^7 - 1607896n^6 + 2420092n^5 + 2017855n^4 + 899112n^3 + 1122697n^2 - 1476508n - 45088.$$

The difference of $p(n+1)$ and $p(n)$ equals

$$p(n+1) - p(n) = 52032n^7 + 254212n^6 - 4243164n^5 - 5193210n^4 + 781934n^3 + 7841885n^2 + 7857749n + 1704480.$$

By Descartes' rule, the number of positive real zeroes of $p(n+1) - p(n)$ is at most 2. Consider

$$\begin{aligned} p(2) - p(1) &= 9055918 > 0, \\ p(3) - p(2) &= -140899954 < 0, \\ p(8) - p(7) &= -10316213144 < 0, \\ p(9) - p(8) &= 16414574600 > 0. \end{aligned}$$

This observation shows that

$$\begin{cases} p(2) > p(1), \\ p(2) > p(3) > \cdots > p(7) > p(8), \\ p(8) < p(9) < \cdots < p(n) < p(n+1) < \cdots. \end{cases}$$

Moreover,

$$\begin{aligned} p(1) &= 3363872, \\ p(3) &= -260324200, \\ p(9) &= -39144733360, \\ p(10) &= 162088321532. \end{aligned}$$

Therefore, we can determine the sign of $a_0^{(5)}$ as follows.

$$a_0^{(5)} \begin{cases} > 0 & (n = 1, 2) \\ < 0 & (3 \le n \le 9) \\ > 0 & (n \ge 10). \end{cases}$$

The remaining cases concerning $a_i^{(k)}$ follow by analogy. □

We can calculate $w(-\infty)$ similarly to the proof of Lemma 5 in such a way that

$$w(-\infty) = \begin{cases} 6 & (1 \le n \le 25) \\ 7 & (26 \le n). \end{cases}$$

Therefore, by combining Lemma 5 with Sturm's theorem, we obtain the following result.

Proposition 1. *The denominator polynomial $D_n(t)$ has the following real roots*:

$$\begin{cases} \text{three positive roots and no negative roots} & (1 \le n \le 25), \\ \text{three positive roots and two negative roots} & (n \ge 26). \end{cases}$$

5.2. The distribution of the complex roots of $D_n(t)$. By applying the method presented in section 3.3, we can deduce an upper bound for the absolute values of all complex roots of $D_n(t)$.

1. Calculate the two real polynomials $\Phi(t)$ and $\Psi(t)$ which are given according to

$$D_n(z(t)) = \frac{\Phi(t) + i\Psi(t)}{(t+i)^{\deg D_n}},$$

where $z(t) = 2\dfrac{t-i}{t+i}$. By using Mathematica, $\Phi(t)$ and $\Psi(t)$ can be written as follows:

$$\Phi(t) = -(162n + 56)t^9 + (6456n - 6512)t^7 - (2476n - 49792)t^5$$
$$- (7176n + 60048)t^3 + (894n + 13752)t,$$
$$\Psi(t) = (2034n - 456)t^8 - (8280n - 24880)t^6 - (7188n + 67136)t^4$$
$$+ (4136n + 36816)t^2 - (14n + 2808).$$

2. By using Mathematica, we can show that the resultant of $\Phi(t)$ and $\Psi(t)$ is not equal to 0 for any $n \in N$. Therefore $D_n(t)$ has no roots on the circle S_2 of radius 2 centered at the origin.

3. By using Mathematica, the Sturm sequence $S(\Phi, \Psi)$ can be calculated.

4. In a manner similar to the argument in section 5.1, we can calculate the numbers of sign changes $w(\infty)$ and $w(-\infty)$ in $S(\Phi, \Psi)$.

Lemma 6. *For any $n \in \mathbf{N}$, $w(\infty) = 8$ and $w(-\infty) = 1$. By Corollary 1, the number of roots of $D_n(t)$ contained in the closed disk of radius 2 centered at the origin in the complex plane $\mathbf{C}$ is equal to 8.*

Theorem 7. *The growth rate of P_n is a Perron number for any $n \in \mathbf{N}$.*

Proof. By Lemma 6, the absolute values of eight roots of $D_n(t)$ are strictly less than 2. Since $\deg D_n(t) = 9$, it is sufficient to prove that $D_n(t)$ has a positive real root which is greater than 2. In order to prove that, we consider $w(2)$. By section 3.3, we obtain

$$w(2) = \begin{cases} 4 & (1 \le n \le 25) \\ 3 & (26 \le n). \end{cases}$$

Therefore, by Sturm's theorem, the polynomial $D_n(t)$ has a unique positive real root which is strictly greater than 2 for any $n \in \mathbf{N}$. □

6. Appendix: the Sturm sequence of $D_n(t)$ and $D_n'(t)$

In this section, we provide the details about the Sturm sequence $S(D_n, D_n') = \{d_0, \dots, d_9\}$ with polynomial ingredients $d_0, \dots, d_9 \in \mathbf{Q}[t]$ given by $(*)$ in section 5.1.

$$\begin{aligned}
d_0(t) &= t^9 - (n+3)t^8 - (n-4)t^7 + (2n-8)t^6 + (2n+8)t^5 + (2n-8)t^4 \\
&\quad - (2n-11)t^3 + (3n-5)t^2 + (3n+4)t - 4(n+1) \\
d_1(t) &= 9t^8 - 8(n+3)t^7 - 7(n-4)t^6 + 6(2n+8)t^5 + 5(2n+8)t^4 \\
&\quad + 4(2n-8)t^3 - 3(2n-11)t^2 + 2(3n-5)t + (3n+4) \\
d_2(t) &= \frac{1}{81}\{(8n^2+66n)t^7 + (7n^2-61n+132)t^6 + (-12n^2-60n-144)t^5 \\
&\quad + (-10n^2-160n+240)t^4 + (-8n^2+116n-498)t^3 \\
&\quad + (6n^2-204n+216)t^2 + (-6n^2-224n-258)t - 3n^2 + 311n + 312\} \\
d_3(t) &= \frac{81}{4n^2(4n+33)^2}\{(39n^4+266n^3-2673n^2-1848n-1936)t^6 \\
&\quad + (36n^4+612n^3+3956n^2+4480n+2112)t^5 \\
&\quad + (54n^4+470n^3-1872n^2-4372n-3520)t^4 \\
&\quad + (-88n^4-776n^3+3866n^2+6246n+7304)t^3 \\
&\quad + (150n^4+1374n^3-3216n^2-1660n-3168)t^2 \\
&\quad + (162n^4+2508n^3+8540n^2+8870n+3784)t \\
&\quad - 259n^4 - 3428n^3 - 7161n^2 - 8548n - 4576\}
\end{aligned}$$

Next, we list the coefficients $a_i^{(k)}$, $0 \le i \le 9-k$, of polynomials $d_k(t)$, $4 \le k \le 8$, according to $(*)$ in section 5.1. We also provide the *denominator* of $d_k(t)$ as given by the least common multiple of coefficients $a_i^{(k)}$.

The denominator of $d_4(t) = 81(1936 + n(1848 + n(2673 - n(266 + 39n))))^2$

$$\begin{aligned}
a_5^{(4)} &= 8n^2(4n+33)^2(270n^6 - 930n^5 - 59765n^4 - 72316n^3 \\
&\quad - 51247n^2 - 34920n + 11920) \\
a_4^{(4)} &= -16n^2(4n+33)^2(51n^6 + 1630n^5 + 7368n^4 - 68445n^3 \\
&\quad - 3176n^2 - 41152n + 16768) \\
a_3^{(4)} &= 8n^2(4n+33)^2(471n^6 + 6452n^5 - 5086n^4 - 176746n^3 \\
&\quad - 54403n^2 - 120344n - 8944)
\end{aligned}$$

$$a_2^{(4)} = 16n^2(4n+33)^2(153n^6 - 411n^5 - 32385n^4 - 33106n^3 - 44007n^2 - 20216n - 7664)$$

$$a_1^{(4)} = -8n^2(4n+33)^2(579n^6 + 14834n^5 + 101041n^4 + 47610n^3 + 25760n^2 + 3472n - 25280)$$

$$a_0^{(4)} = 16n^2(33+4n)^2(10304 + 60992n + 92088n^2 + 112317n^3 + 78944n^4 + 5932n^5 + 33n^6)$$

The denominator of $d_5(t) = 4n^2(33+4n)^2(11920 - 34920n - 51247n^2 - 72316n^3 - 59765n^4 - 930n^5 + 270n^6)^2$

$$a_4^{(5)} = -81(39n^4 + 266n^3 - 2673n^2 - 1848n - 1936)^2(246n^8 - 5794n^7 + 360959n^6 + 5606880n^5 - 3313218n^4 + 6140122n^3 - 3491843n^2 + 2584756n - 544176)$$

$$a_3^{(5)} = 162(39n^4 + 266n^3 - 2673n^2 - 1848n - 1936)^2(5289n^8 + 5992n^7 - 788952n^6 - 810030n^5 - 5107313n^4 + 118907n^3 - 2823408n^2 + 1353973n - 43828)$$

$$a_2^{(5)} = -81(39n^4 + 266n^3 - 2673n^2 - 1848n - 1936)^2(8442n^8 - 32742n^7 - 1868957n^6 - 1946748n^5 - 4253223n^4 - 1203496n^3 - 1818280n^2 + 440564n - 127008)$$

$$a_1^{(5)} = -162(39n^4 + 266n^3 - 2673n^2 - 1848n - 1936)^2(6261n^8 + 27352n^7 - 543939n^6 + 1168425n^5 - 740209n^4 - 333809n^3 - 454006n^2 - 793981n + 269220)$$

$$a_0^{(5)} = 81(39n^4 + 266n^3 - 2673n^2 - 1848n - 1936)^2(13008n^8 + 20600n^7 - 1607896n^6 + 2420092n^5 + 2017855n^4 + 899112n^3 + 1122697n^2 - 1476508n - 45088)$$

The denominator of $d_6(t) = 81(-1936 - 1848n - 2673n^2 + the266n^3 + 39n^4)^2 (-544176 + 2584756n - 3491843n^2 + 6140122n^3 - 3313218n^4 + 5606880n^5 + 360959n^6 - 5794n^7 + 246n^8)^2$

$$a_3^{(6)} = -8n^2(4n+33)^2(270n^6 - 930n^5 - 59765n^4 - 72316n^3 - 51247n^2 - 34920n + 11920)^2(403481n^{10} + 2480778n^9 - 37969219n^8 - 158119702n^7$$

$$- 1100390746n^6 - 216055166n^5 - 1160964773n^4 + 282443786n^3 - 329580155n^2 + 172728524n - 35052620)$$

$$a_2^{(6)} = 16n^2(4n+33)^2(270n^6 - 930n^5 - 59765n^4 - 72316n^3 - 51247n^2 - 34920n + 11920)^2(169494n^{10} + 14649n^9 - 18830064n^8 + 62828800n^7 - 387398843n^6 + 226406803n^5 - 413299018n^4 + 245275527n^3 - 138927361n^2 + 67186063n - 4007124)$$

$$a_1^{(6)} = 8n^2(4n+33)^2(270n^6 - 930n^5 - 59765n^4 - 72316n^3 - 51247n^2 - 34920n + 11920)^2(474903n^{10} + 4516538n^9 - 11601465n^8 + 104831670n^7 + 294141284n^6 - 180768204n^5 + 111338775n^4 - 296355112n^3 + 31452859n^2 - 39181768n + 10452012)$$

$$a_0^{(6)} = -16n^2(4n+33)^2(270n^6 - 930n^5 - 59765n^4 - 72316n^3 - 51247n^2 - 34920n + 11920)^2(252601n^{10} + 1535932n^9 - 10172760n^8 + 137682333n^7 + 130244020n^6 + 208421539n^5 + 143139607n^4 + 2115857n^3 + 44003972n^2 - 41200307n + 18745192)$$

The denominator of $d_7(t) = 4n^2(33+4n)^2(11920 - 34920n - 51247n^2 - 72316n^3 - 59765n^4 - 930n^5 + 270n^6)^2(-35052620 + 172728524n - 329580155n^2 + 282443786n^3 - 1160964773n^4 - 216055166n^5 - 1100390746n^6 - 158119702n^7 - 37969219n^8 + 2480778n^9 + 403481n^{10})^2$

$$a_2^{(7)} = 81(39n^4 + 266n^3 - 2673n^2 - 1848n - 1936)^2(246n^8 - 5794n^7 + 360959n^6 + 5606880n^5 - 3313218n^4 + 6140122n^3 - 3491843n^2 + 2584756n - 544176)^2(48400755n^{12} + 245803454n^{11} - 4721345357n^{10} - 11572421870n^9 - 124324436353n^8 - 146160412422n^7 - 206861074257n^6 - 134297550268n^5 - 66775078001n^4 - 24225751096n^3 + 3620403819n^2 - 813838328n + 111404496)$$

$$a_1^{(7)} = 162(39n^4 + 266n^3 - 2673n^2 - 1848n - 1936)^2(246n^8 - 5794n^7 + 360959n^6 + 5606880n^5 - 3313218n^4 + 6140122n^3 - 3491843n^2 + 2584756n$$

$$- 544176)^2(9127365n^{12} + 43738914n^{11} - 1050600669n^{10} - 2134594907n^9$$
$$- 221052668n^8 + 8764159647n^7 + 11937399782n^6 + 16709700491n^5$$
$$+ 4028829086n^4 + 2954840024n^3 - 2598459169n^2 - 405956928n$$
$$- 67672272)$$

$$a_0^{(7)} = -81(39n^4 + 266n^3 - 2673n^2 - 1848n - 1936)^2(246n^8 - 5794n^7 + 360959n^6$$
$$+ 5606880n^5 - 3313218n^4 + 6140122n^3 - 3491843n^2 + 2584756n$$
$$- 544176)^2(59130903n^{12} + 320783028n^{11} - 5921870437n^{10}$$
$$- 16668405100n^9 - 117418503841n^8 - 151967821848n^7 - 180213457131n^6$$
$$- 140644288440n^5 - 51131969275n^4 - 32331152680n^3 + 5676560341n^2$$
$$- 2814520288n - 23940048)$$

The denominator of $d_8(t) = 81(-1936 - 1848n - 2673n^2 + the266n^3 + 39n^4)^2$

$$(-544176 + 2584756n - 3491843n^2 + 6140122n^3$$
$$- 3313218n^4 + 5606880n^5 + 360959n^6 - 5794n^7$$
$$+ 246n^8)^2(111404496 - 813838328n$$
$$+ 3620403819n^2 - 24225751096n^3 - 66775078001n^4$$
$$- 134297550268n^5 - 206861074257n^6$$
$$- 146160412422n^7 - 124324436353n^8$$
$$- 11572421870n^9 - 4721345357n^{10} + 245803454n^{11}$$
$$+ 48400755n^{12})^2$$

$$a_1^{(8)} = 16n^2(4n + 33)^2(270n^6 - 930n^5 - 59765n^4 - 72316n^3 - 51247n^2 - 34920n$$
$$+ 11920)^2(403481n^{10} + 2480778n^9 - 37969219n^8 - 158119702n^7$$
$$- 1100390746n^6 - 216055166n^5 - 1160964773n^4 + 282443786n^3$$
$$- 329580155n^2 + 172728524n - 35052620)^2(1462545045n^{14}$$
$$- 10472627469n^{13} - 402243294759n^{12} - 1104112693071n^{11}$$
$$- 8571517376059n^{10} - 16797900884717n^9 - 22904507347277n^8$$
$$- 22168784110521n^7 - 14235620251809n^6 - 6907194126551n^5$$
$$- 2062300172501n^4 - 196719185377n^3 - 72614586920n^2$$
$$+ 4391952n - 226865664)$$

$$
\begin{aligned}
a_0^{(8)} = &-16n^2(4n+33)^2(270n^6-930n^5-59765n^4-72316n^3-51247n^2-34920n\\
&+11920)^2(403481n^{10}+2480778n^9-37969219n^8-158119702n^7\\
&-1100390746n^6-216055166n^5-1160964773n^4+282443786n^3\\
&-329580155n^2+172728524n-35052620)^2(682442280n^{14}\\
&-13967744415n^{13}-318617986273n^{12}-866028050552n^{11}\\
&-5973136686946n^{10}-11470936502501n^9-15278417145211n^8\\
&-15018314214172n^7-9591556809634n^6-5038052836203n^5\\
&-1582742665577n^4-286371055374n^3-76587929392n^2\\
&-3723242592n-226865664)
\end{aligned}
$$

Finally, we give the details of $d_9 = d_9(n) \in \mathbf{Q}$.

$$
\begin{aligned}
\text{The numerator of } d_9 = \; &81(39n^4+266n^3-2673n^2-1848n-1936)^2\\
&(246n^8-5794n^7+360959n^6+5606880n^5-3313218n^4\\
&+6140122n^3-3491843n^2+2584756n-544176)^2\\
&(48400755n^{12}+245803454n^{11}-4721345357n^{10}\\
&-11572421870n^9-124324436353n^8-146160412422n^7\\
&-206861074257n^6-134297550268n^5-66775078001n^4\\
&-24225751096n^3+3620403819n^2-813838328n\\
&+111404496)^2(36591985143n^{15}-329358176568n^{14}\\
&-12543536009205n^{13}-52547213609708n^{12}\\
&-300328073161252n^{11}-864495115585896n^{10}\\
&-1442487093482529n^9-1706342509194068n^8\\
&-1467752091940232n^7-887326796059424n^6\\
&-391684164932313n^5-109950671986036n^4\\
&-10905495292115n^3-4664082142496n^2\\
&-93566282832n-10889551872)
\end{aligned}
$$

$$
\begin{aligned}
\text{The denominator of } d_9 = \; &4n(4n+33)^2(270n^6-930n^5-59765n^4-72316n^3\\
&-51247n^2-34920n+11920)^2(403481n^{10}+2480778n^9\\
&-37969219n^8-158119702n^7-1100390746n^6
\end{aligned}
$$

$$
\begin{aligned}
&- 216055166n^5 - 1160964773n^4 + 282443786n^3 \\
&- 329580155n^2 + 172728524n - 35052620)^2 \\
&(1462545045n^{14} - 10472627469n^{13} - 402243294759n^{12} \\
&- 1104112693071n^{11} - 8571517376059n^{10} \\
&- 16797900884717n^9 - 22904507347277n^8 \\
&- 22168784110521n^7 - 14235620251809n^6 \\
&- 6907194126551n^5 - 2062300172501n^4 \\
&- 196719185377n^3 - 72614586920n^2 + 4391952n \\
&- 226865664)^2
\end{aligned}
$$

7. Acknowledgements

The author wishes to express his gratitude to Professor Ruth Kellerhals and Professor Yohei Komori for fruitful discussions and helpful comments around Sturm's theorem. This work was partially supported by Grant-in-Aid for JSPS Fellows number 17J05206.

References

[1] J. W. Cannon and P. Wagreich, Growth functions of surface groups, Math. Ann. **293** (1992), 239–257.
[2] P. M. Cohn, Basic Algebra: groups, rings, and fields., Springer-Verlag, London, 2003.
[3] W. J. Floyd, Growth of planer Coxeter groups, P.V. numbers, and Salem numbers, Math. Ann. **293** (1992), 475–483.
[4] T. W. Gamelin, Complex analysis, Undergraduate texts in mathematics, Springer-Verlag, New York, 2001.
[5] P. de la Harpe, Groupes de Coxeter infinis non affines, Exposition. Math. **5** (1987), 91–96.
[6] J. E. Humphreys, Reflection groups and Coxeter groups, Cambridge studies in advanced mathematics **29**, Cambridge Univ. Press, Cambridge, 1990.
[7] R. Kellerhals and G. Perren, On the growth of cocompact hyperbolic Coxeter groups, European J. Combin. **32** (2011), 1299–1316.
[8] A. Kolpakov, Deformation of finite-volume hyperbolic Coxeter polyhedra, limiting growth rates and Pisot numbers, European J. Combin. **33** (2012), 1709–1724.
[9] A. Kolpakov and A. Talambutsa, Spherical and geodesic growth rates of right-angled Coxeter and Artin groups are Perron numbers, arXiv:1809.09591.
[10] Y. Komori and T. Yukita, On the growth rate of ideal Coxeter groups in hyperbolic 3-space, Proc. Japan Acad. Ser. A. Math. Sci. **91** (2015), 155–159.
[11] L. Kronecker, Über die verschiedenen Sturm'schen Reihen und ihre gegenseitigen Beziehungen, Ber. K. Acad. Wiss. Berlin (1873), 117–154, Leopold Kronecker's Werke **1**, Chelsea Publishing Company, New York, 1968, 303–348.

[12] J. Nonaka and R. Kellerhals, The growth rates of ideal Coxeter polyhedra in hyperbolic 3-space, Tokyo J. of Math. **40** (2017), 379–391.
[13] W. Parry, Growth series of Coxeter groups and Salem numbers, J. Algebra **154** (1993), 406–415.
[14] V. V. Prasolov, Polynomials, Algor. Comput. in Math. **11**, Springer, Berlin, 2004.
[15] J. G. Ratcliffe, Foundations of hyperbolic manifolds, Grad. texts in math. **149**, Springer, New York, 1994.
[16] L. Solomon, The orders of the finite Chevalley groups, J. Algebra **3** (1966), 376–393.
[17] R. Steinberg, Endomorphisms of linear algebraic groups, Memoirs of the American Mathematical Society **80**, Amer. Math. Soc., Providence, RI, 1968.
[18] P. V. Tumarkin, Hyperbolic Coxeter n-polytopes with $n+3$ facets, Trans. Moscow. Math. Soc. (2004), 235–250.
[19] Y. Umemoto, The growth function of Coxeter dominoes and 2-Salem numbers, Algebr. Geom. Topol. **14** (2014), 2721–2746.
[20] E. B. Vinberg, Geometry. II; Spaces of constant curvature, Encycl. math. sci. **29**, 1993.
[21] T. Yukita, On the growth rates of cofinite 3-dimensional hyperbolic Coxeter groups whose dihedral angles are of the form $\frac{\pi}{m}$ for $m = 2, 3, 4, 5, 6$, RIMS Kôkyûroku Bessatsu **B66** (2017), 147–165.
[22] T. Yukita, Growth rates of 3-dimensional hyperbolic Coxeter groups are Perron numbers, Canad. Math. Bull. **61** (2018), 405–422.
[23] T. Zehrt and C. Zehrt, The growth function of Coxeter garlands in $\mathbf{H}^4$, Beitr. Algebra Geom. **53** (2012), 451–460.

Tomoshige Yukita
Department of Mathematics
School of Education
Waseda University
Nishi-Waseda 1-6-1, Shinjuku
Tokyo 169-8050
Japan
E-mail: yshigetomo@suou.waseda.jp